International Journal of Multidisciplinary Research and Development
Online ISSN: 2349-4182, Print ISSN: 2349-5979, Impact Factor: RJIF 5.72
www.allsubjectjournal.com
Volume 3; Issue 4; April 2016; Page No. 117-124

Dynamic behaviour of SIC particulate reinforced polymer composite beam

[1] Nityananda Biswal, *[2] Pankaj Charan Jena, [3] R C. Mohanty
[1, 3] Department of Mechanical Engineering, Centurion University of Technology & Management, Bhubaneswar, India
[2] Department of Mechanical Engineering, Orissa Engineering College, Bhubaneswar, India

Abstract
The aim of the current research is to design a micro-scaled particulate fibre reinforced polymer (PRP) composite beam type structure having improved specific weight density and stiffness and studying the vibration characteristics of the designed PRP beams. In the present investigation, epoxy resin is used as matrix or binder and micro-scaled particulate Silicon carbide fibres are used for reinforcement in epoxy resins in presence of catalyst. The mode shape and frequency of the PRP composite beams are obtained using two approaches (theoretical approach and finite element approach). These responses subsequently compare with actual experiments performed on composite beam manufactured in the laboratory. An effort has been made to examine the vibration parameters with respect to weight percentage of Silicon Carbide reinforcement in epoxy resins as it changes the stiffness of composite beams. The vibration parameters are frequency, and corresponding mode shape with varying fibre weight percentage. The deviation of results among the three methods is also computed and it is observed the results are varied from 0% to 5%.

Keywords: SiC-particulate, epoxy, composite, beam, stiffness, vibration.

1. Introduction
To overcome these limitations of conventional materials, the researchers are focused on an alternative composite material with enhanced material properties. The composite materials are provided low specific weight density, higher stiffness, good surface finish so that it looks attractive. Therefore, in this present investigation the various techniques are proposed and designed with an aim to obtain an alternative composite material which is addressed the good mechanical properties and applications in dynamical surrounding. This investigation is exploring the various methods like composite fabrication techniques, numerical analysis, finite elment analysis and experimental analysis of prepared particulate composite beams. Previous researchers have presented different methods to prepare particulate composite materials and mechanical formulations for finding properties with refer to weight fraction of fibers and matrix in composite materials [1-5]. The mathematical derivations have derived for composite beam/plate in dynamic surroundings considering various load conditions like axial loading, bending moment, and shear force [6]. the mixture formulae to get the various physical and mechanical properties for different fiber fraction in composite materials have given [6]. The different techniques have presented about the manufacture process of composite material [7]. The design, synthesis, and characterization of Polymer-ceramic nano-composites have discussed [8]. a new class of material has presented which is based on smetite class usually rendered hydrophobic through ionic exchange of the sodium interlayer cation with an onium cation. i.e. (Polymer-layered silicate nanocomposite) they found exhibits enhanced property even at very lower filler level. Such as Young's modules, storage modules thermal stabilities, Gas barrier Properties & Good Flam resistance [9]. The design and laboratory setup have illustrated to prepare nano-composite material [10]. They have synthesized nano-composite material by doping SiC in epoxy resin at room temperature. During the preparation of mixture they have used vacuum transfer molding technique. They have investigated mechanical properties and impact test at low velocity on it. They have found enhance of mechanical properties. They have also observed that by infusion of nano size Si C particles, the samples exhibit high rates of strain. the effect of moisture in mechanical properties of carbon/epoxy composite materials have found experimentally for bidirectional composites ([0/90]s and [±45]s) leads to a lower rate of moisture absorption as compared to unidirectional reinforced composites due to the edges effect [11]. The comparative performance of glass-epoxy composite system interfaced with graded fillers has been examined and used a Pin-on-Disc type wear tester for investigation of composite material under varying load and sliding velocity [12]. It was observed that the graphite filled G.E composite shows lower coefficients of friction than the other two composites irrespective of variation in the load/sliding velocity. Among the different filler material, they have observed Si C filled G-E composite exhibited the max wear Resistance. The fatigue life and ageing of polymer composite material by non-destructive method have numerically modeled the equation using finite element method and simulated dynamic acoustic under thermal surroundings and studied the changes of physical properties of composite structure like stiffness, acoustic wave propagation velocity and thermal conductivity under the model structural and parametric modifications [13]. The moisture absorbed behavior of polymer composite in humidity and tropical surroundings have found that Vinylester/carbon samples shown better to epoxy/carbon in all the test conditions [14]. The combined carbon nanofibers and microsized short carbon fibres on epoxy leads to significant improvement in the mechanical properties of the matrix have studied [15]. It was revealed that the combined use of SCFs and silica the nanoparticles exerts a synergetic effect on the mechanical properties and fracture properties of Epoxy. It has observed during experimental process that the particles were synthesized by a sequential

reversible addition-fragmentation chain transfer (RAFT) polymerization and the inner rubbery block poly (n-hexyl methacrylate) (PHMA) had a glass transition temperature below room temperature [16]. The outer block poly (glycidyl methacrylate) (PGMA) was matrix compatible. Both systems enabled cavitation or plastic dilatation. Improvement of the strain-to-break and the tensile toughness was found in both systems. The investigations have done on alternative composite armor plate which is provided resistance to bullet fired from arm weapons and they have investigated this proving resistance in epoxy glass fabric composite sheets by punching and destructive techniques[17]. The comparision has carried out with the natural fiber reinforced polymer composites with the glass fiber reinforced polymer composite and they conclude that NFRPS is the alternative to SFRPS in many applications for their many advantages [18]. They were studied the effect of weight fraction of nanoparticles on mechanical behavior of silica-epoxy nanocomposites and they got the following conclusions: (1) Increasing of Young's modulus, tensile stress, and yield stress with rigid particles and these values are decreased for soft particle, (2) the tensile strengths, compressive strengths, Young's modulus, flexural strength, flexural modulus and fracture toughness increases with increasing of particle loading[19-24]. In experimentally, they have found that the thermal conductivity of epoxy/AgNWs@Sio2 composite is higher than those epoxy/ AgNWs composite with the same loading [25].

The mathematical expressions have presented for vibration of beam with different boundary conditions and have studied the various beam structures behavior in dynamical surroundings and their vibration parameters under different boundary conditions and loading. They worked on vibration behavior of fiber reinforced composite beam. They have stated the fiber distribution and orientation have a role on mechanical properties as well as stiffness of the composite beam. They have used finite element method to learn the vibration mode shape and natural frequency of composite beam. Further they have successfully applied the finite element method to examine the vibration parameters of aluminium metal matrix composite + SiC produced in plunger techniques [26-29].

The aim of the current research is to design a micro-scaled particulate fibre reinforced polymer (MPFRP) composite beam type structure having improved specific weight density and stiffness and studying the vibration characteristics of the designed MPFRP beams. In the present investigation, epoxy resin is used as matrix or binder and micro-scaled particulate Silicon carbide particulate (size is shown in Fig.2) are used for reinforcement in epoxy resins in presence of catalyst. The mode shape and frequency of the MPFRP composite beams are obtained using two approaches (theoretical approach and finite element approach). These responses subsequently compare with actual experiments performed on composite beam manufactured in the laboratory. The vibration parameters are amplitude, frequency, and corresponding mode shape with varying fibre weight percentage.

2. Preparation of the Test Specimens

The fixed amount of epoxy resin with different weight percentages of SiC (10%wt, 15%wt, 20% wt and 25% wt, 30% wt) are considered for preparation of particulate reinforced composite materials in present study. In this investigation SiC particles of each weight percentage are suspended in 326gm of epoxy resin in different container. By help of stirrer, the each mixture is stirred for 30 minutes to get compete uniform distributed particles inside the resin. After getting uniform mixture, the solution is left 30 minutes on vibrator/sacker to remove air bubbles and voids shown in Fig.1. Then the mixture is spread out uniformly over the mould in presence of catalyst. This process is repeated till get the all specimens. No external pressure is applied during casting or curing as uncured matrix material can squeeze out under high pressure. This causes surface waviness (non-uniform thickness) and roughness in the model material. The casting is cured at room temperature for 6 hours and finally removed from the bed (mould) to get a fine finished composite plate. After the curing process, test specimens are obtained of size 600 mm x 40 mm x 5 mm.

Fig 1: Preparation of Test Specimen with Glass Mould.

Fig 2: SiC particulate fibres with particle size 343micron.

3.6 Material Properties of particulate composite obtained from various Tests,

Table 1: Mechanical properties of particulate (powder form) composite beams using Experimental Test.

Mechanical properties	Epoxy + 0% SiC	Epoxy + 10% SiC	Epoxy + 15% SiC	Epoxy + 20% SiC	Epoxy + 25% SiC	Epoxy + 30% SiC
young's modulus (MPa)	385.34	429.1068	465.562	605.952	784.584	819.783
Poisson's ratio	3.24	3.2	3.12	3.03	2.9	2.86
Density (kg/m^3)	1220	1285.12	1285.12	1285.12	1285.12	1285.12

Table 2: Mechanical properties of particulate (60 mesh size) composite beams using Experimental Test.

Mechanical properties	Epoxy + 0% SiC	Epoxy + 10% SiC	Epoxy + 15% SiC	Epoxy + 20% SiC	Epoxy + 25% SiC	Epoxy + 30% SiC
young's modulus (MPa)	385.34	449.1068	535.562	625.952	804.6	910.913
Poisson's ratio	3.24	3.22	3.11	3.01	2.92	2.83
Density (kg/m^3)	1220	1466.66	1466.66	1466.66	1466.66	1466.66

3. Vibration Analysis

This work deals with the SiC particle (60 mesh size) reinforcement in epoxy as polymer matrix to prepare micro-scaled-particulate composite beams which has been discussed in Chapter 3. Further, these micro-scaled-particulate composite beams are used for dynamic analysis under free vibration with different boundary conditions.

To determine the differential equation for lateral vibration of micro-scaled-particulate composite beam, consider the forces and bending moments acting on an element of the micro-scaled-particulate composite beam shown in Fig. 3. Let, V and M are shear force and bending moments at left side of the micro-scaled-particulate composite beam element and $P(x)$ represents the loading per unit length of the micro-scaled-particulate composite beam. V+dV and M+dM are increased shear force and bending moments at right side of the micro-scaled-particulate composite beam element.

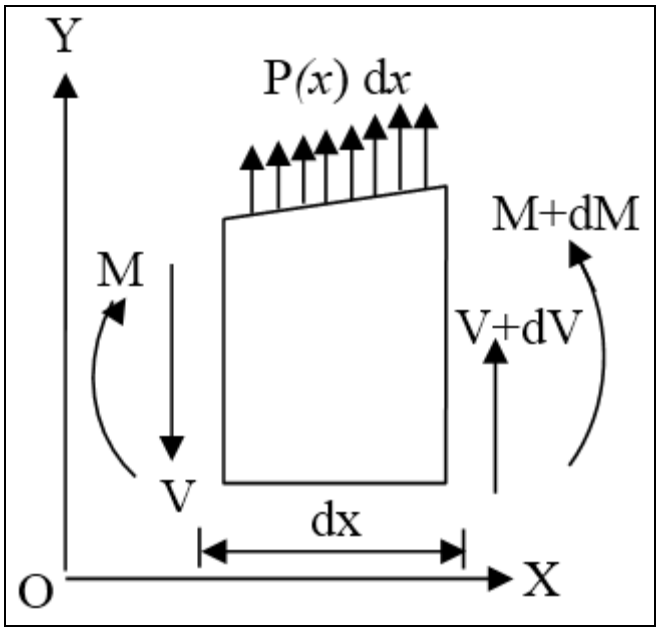

Fig 3: Beam element of length dx with transverse load per unit length, Bending moment and shear force.

Now by summing forces in Y- direction,

$$d V \_ P(x)dx = 0 \quad (1)$$

By summing moments about any point on the right face of the element,

$$dM \_ Vdx \_ P(x)dx\left(\frac{dx}{2}\right) = 0 \quad (2)$$

$$\Longrightarrow dM \_ Vdx \_ [\frac{1}{2}[P(x)(dx)^2] = 0 \quad (2a)$$

In the limiting process these equations result in the following important relationships,

$$\frac{dV}{dx} = P(x); \qquad \frac{dM}{dx} = V \quad (3)$$

The first part of the equation (3) states that the rate of change of shear force along the length of the micro-scaled-particulate composite beam is equal to the loading per unit length.

The second states that the rate of change of the moment along the micro-scaled-SiC particulate composite beam is equal to the Shear force.

From equation (3), we obtain the following

$$\frac{d^2M}{dx^2} = \frac{dV}{dx} = P(x) \quad (4)$$

The bending moment is related to the curvature by the flexure equation, which, for the coordinates indicated in the Figure 1.

$$M = EI\frac{d^2Y}{dx^2} \quad (5)$$

Substitute this relation into equation (4) we obtain,

$$\frac{d^2}{dx^2}\left(EI\frac{d^2Y}{dx^2}\right) = P(x) \quad (6)$$

For a beam vibrating about its static equilibrium position under its own weight, the load per unit length is equal to the inertia load due to its mass and acceleration. Since the inertia force is the same direction as$P(x)$, as shown in figure, we have, by assuming harmonic motion,

$$P(x) = \rho\omega^2 y \quad (7)$$

Where, ρ is the mass per unit length of the beam?

Using this relation, the equation for the lateral vibration of the beam reduces to

$$\frac{d^2}{dx^2}\left(EI\frac{d^2Y}{dx^2}\right) - \rho\omega_n^2 y = 0 \quad (8)$$

In the special case where the flexural rigidity EI is constant, the above equation may be written as, $\left(EI\frac{d^4Y}{dx^4}\right) - \rho\omega_n^2 y = 0$ (9)

On substituting, $\beta^4 = \frac{\rho\omega_n^2}{EI}$ (10)

We obtain the fourth- order differential equation,

$$\frac{d^4Y}{dx^4} - \beta^4 y = 0 \quad (11)$$

For the vibration of a uniform beam,

The general solution of equation (11) can be shown to be

$$Y = A\cosh\beta x + B\sinh\beta x + C\cos\beta x + D\sin\beta x \quad (12)$$

To arrive at this result, we assume a solution of the form

$$Y = e^{ax} \quad (13)$$

Which will satisfy the differential equation when, $a = \pm\beta, and\ a = \pm i\beta$

Since, $e^{\pm\beta x} = \cosh\beta x \pm \sinh\beta x$ so, $e^{\pm i\beta x} = \cos\beta x \pm i \sin\beta x$ the solution in the form of equation (12) readily established.

The natural frequencies of vibration are found from equation (10) to be

$$\omega_n = \beta_n^2 \sqrt{\frac{EI}{\rho}} = (\beta_n l)^2 \sqrt{\frac{EI}{\rho l^4}} \quad (14)$$

Where the β depends on the boundary conditions of the beam.

4. Experimental Analysis:

The accelerometer (vibration response pick up) is placed on the PRP composite beam to capture vibration parameters. In order to capture the dynamic response (first three natural frequencies and corresponding mode shapes) of PRP composite beam in the experiment, the exciter (power hammer) and the function generator are employed to make initial excitation in the PRP composite beams. After initial excitation, the signals are sensed by accelerometer and the signal is passed to the FFT analyzer. The FFT analyzer consists of Pulse PC card I/P and PC interfaced PULSE LITE software and connected to display unit. From this, the first three natural frequencies and corresponding mode shapes of PRP composite are drawn. The detail experiment setup is presented in Fig.4.

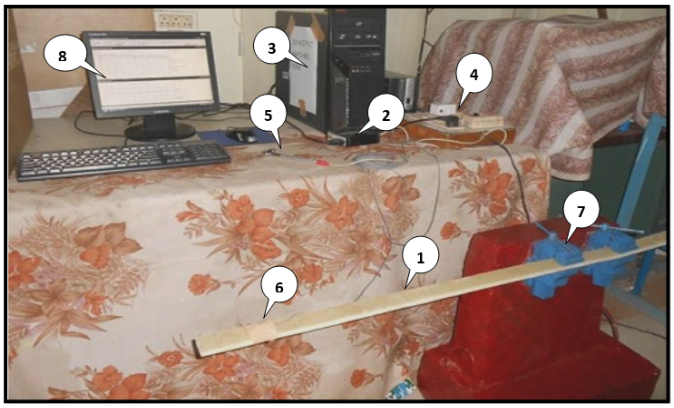

Fig 4: Experimental setup. 1-PRP beam; 2-Vibration analyzer; 3-PC interface PULSELITE software; 4-Power supply; 5-Power hammer; 6-Accelerometer; 7-clamp; 8-Vibration indicator.

5. Finite Element Approach Using ANSYS

In addition to the theoretical approach, finite element approach (FEA) is used using ANSYS (release version 13) to determine natural frequencies and mode shapes of PRP composite beam[30]. For the analysis, the dimension of the PRP composite beam is taken as 640 mm × 50 mm × 6 mm comprising of eleven layers. Each layer is a combination of Epoxy resins (matrix) and SiC particulate (fibre). In order to model the PRP beam, 8 nodded solid elements are used.

Mechanical properties of the composite beam are obtained from various tests performed on the PRP composite material. The detail of the procedure is mentioned in the experimental procedure section. The beam models are meshed and the boundary conditions are set as per the end conditions (clamped-free). From modal solutions, natural frequencies and mode shapes are computed separately for PRP composite beam. The changes in mode shapes are plotted by varying weight fraction (10%, 15%, 20%, 25% and 30%) of SiC particle in composite beam. The frequency (ω_n) of PRP beam is computed.

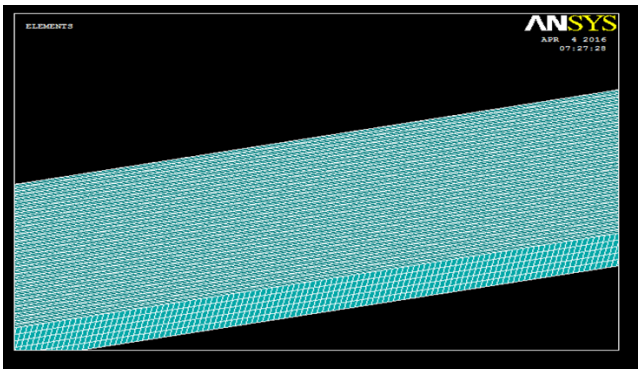

Fig 5: meshing model of PRP composite beam.

6. Results and Discussions

Using theoretical approach and experimental technique, the vibration characteristics namely first, second, and third natural frequencies as well as corresponding mode shapes are obtained for PRP composite beams with weight percentage of SiC. Fig. 4 shows an experimental model of PRP beam with clamp-free end condition. Natural frequency and corresponding mode shape are calculated with varying the boundary conditions. Effect of weight percentage of SiC+epoxy composite beam in dynamic character is also studied. A numerous PRP composite beam are examined in order to obtain the vibration response (first three natural frequencies and corresponding mode shape curvature) by altering the weight percentage of SiC. Theoretical and experiment verifications are conducted with the different weight percentage of SiC of PRP beam for clamped-free and clamped-clamped boundary conditions. The Experiments are conducted by varying weight percentage of SiC. Experimental setup used to determine the frequency and mode shape are shown in Fig. 4. For result analysis, the natural frequency of PRP beam **ω** is computed. The mode shapes of PRP beam are compared among the theoretical and experimental results in this chapter with different boundary conditions by altering the weight percentage of SiC. From these mode shapes, few are shown in the Figures 5 to 13. The Figures 14 to 16 present the frequency and corresponding mode shape which are obtained from ANSYS. Furthermore, the obtained FEA results are compared with the results of experimental and analytical analysis in table 3. From these Figures, it is established that mode shape curvature have significantly affected by altering the weight percentage of SiC. The natural frequency and corresponding mode shape achieved from experiment by varying weight percentage of SiC have been compared with results of the theoretical analysis. The comparison graphs are shown in Figures 5 to 13.

Few comparison results in non-dimensional form of frequencies are depicted in Tables 3 which show good agreement (error within 5%) with the results of the experiment, FEA and theoretical investigations. The non-dimensional form of frequencies are computed as $\frac{\omega_0}{\omega}$ where ω presents

natural frequency of PRP composite beam with SiC particulate and ω_0 presents natural frequency of PRP composite beam with 0% SiC particulate. The error percentage is computed as $\left(\frac{\omega-\omega_0}{\omega}\right)\times 100$. The Figures 17 to 19 present the comparisons among non-dimensional natural frequencies which are obtained from three characterizing methods (theoretical, FEA, experiment) of Clamped-Free PRP beam with respect to weight percentage of SiC particulate reinforcement.

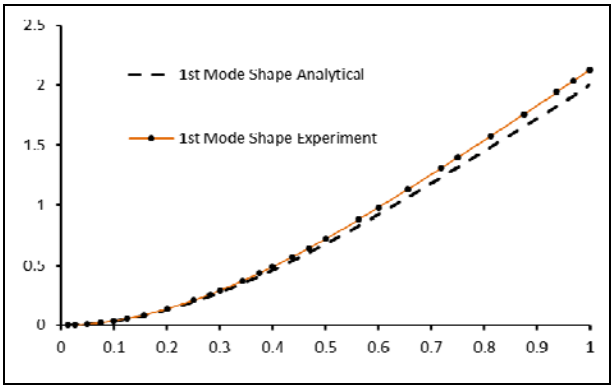

Fig 5: comparison of first mode shape of clamped-free PRP composite beam between analytical method and experimental methods at 10% Si C.

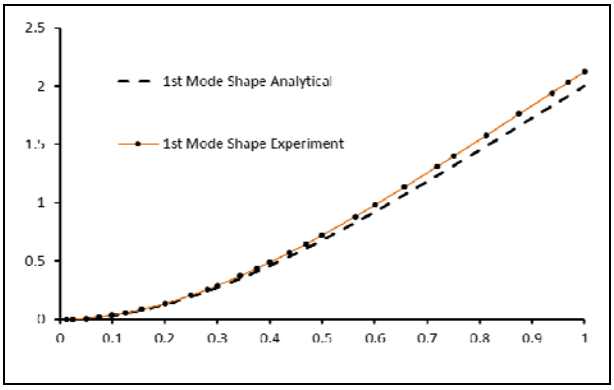

Fig 6: comparison of first mode shape of clamped-free PRP composite beam between analytical method and experimental methods at 20% Si C.

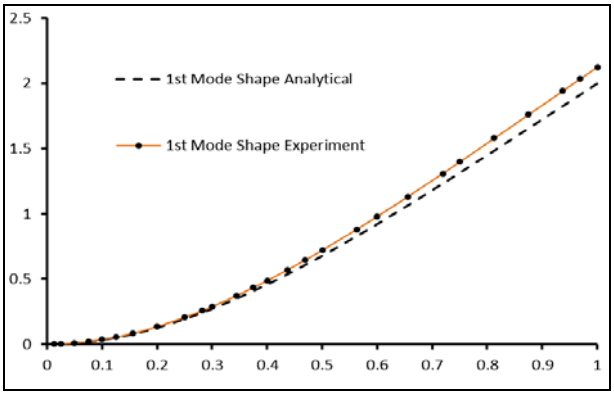

Fig 7: comparison of first mode shape of clamped-free PRP composite beam between analytical method and experimental methods at 30% Si C.

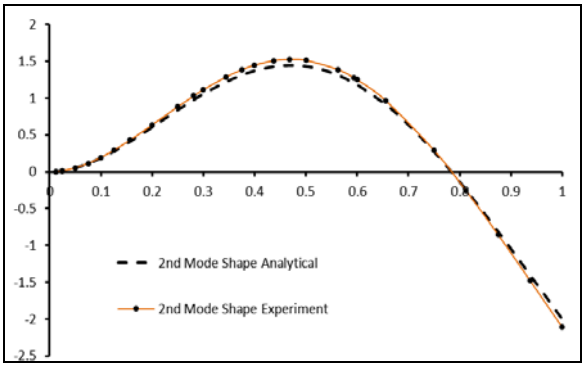

Fig 8: comparison of second mode shape of clamped-free PRP composite beam between analytical method and experimental methods at 10% SiC.

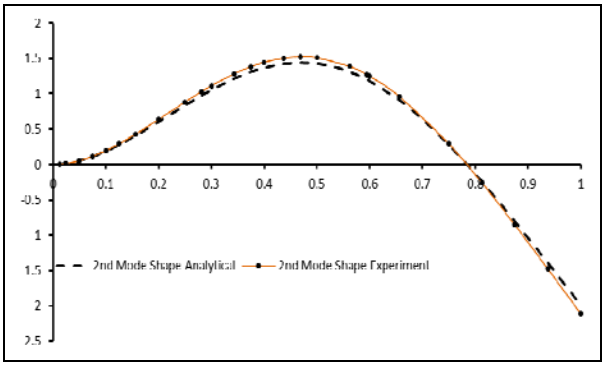

Fig 9: comparison of second mode shape of clamped-free PRP composite beam between analytical method and experimental methods at 20% SiC.

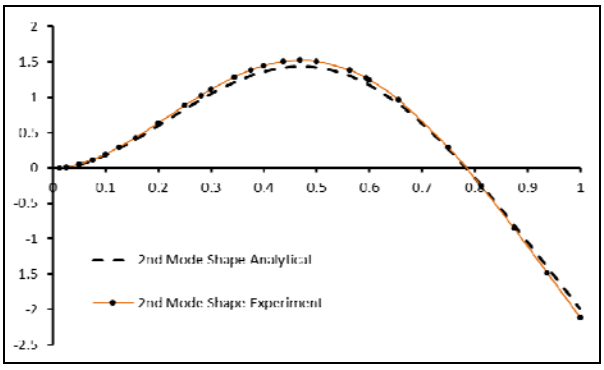

Fig 10: comparison of second mode shape of clamped-free PRP composite beam between analytical method and experimental methods at 30% Si C.

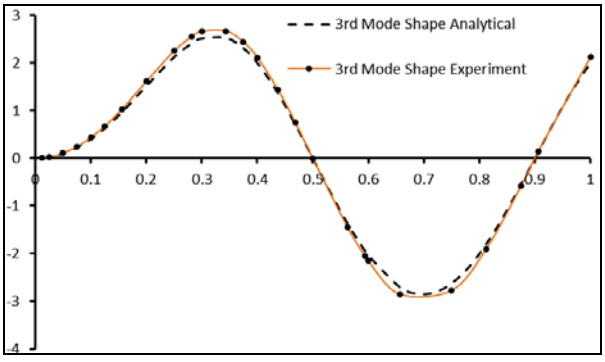

Fig 11: comparison of third mode shape of clamped-free PRP composite beam between analytical method and experimental methods at 10% Si C.

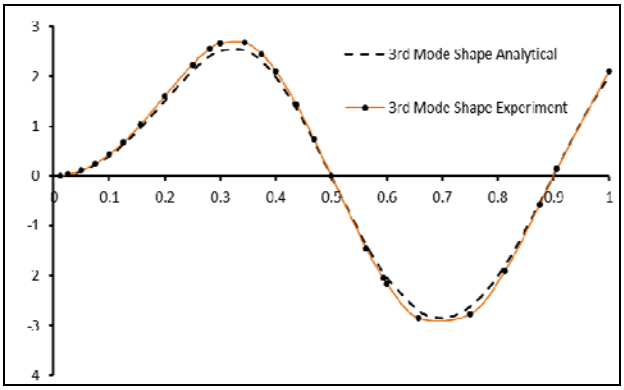

Fig 12: comparison of third mode shape of clamped-free PRP composite beam between analytical method and experimental methods at 20% Si C.

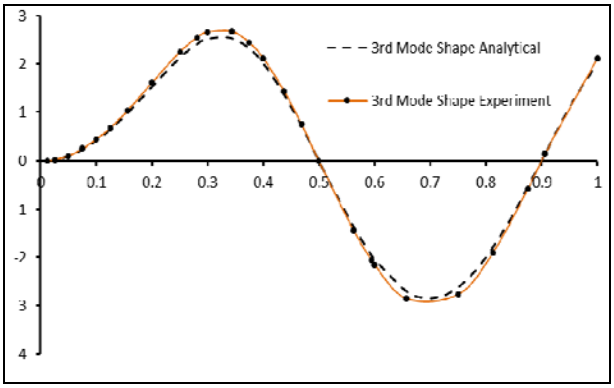

Fig 13: comparison of third mode shape of clamped-free PRP composite beam between analytical method and experimental methods at 30% Si C.

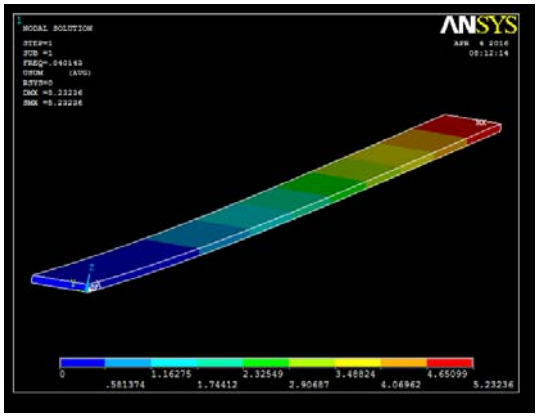

Fig 14: first mode shape of C-F PRP beam at 10% Si C.

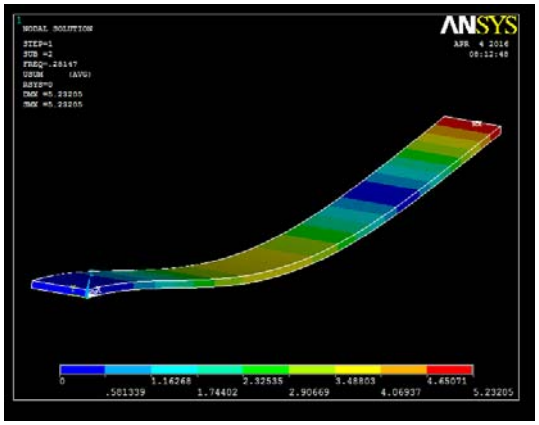

Fig 15: second mode shape of C-F PRP beam at 10% SiC.

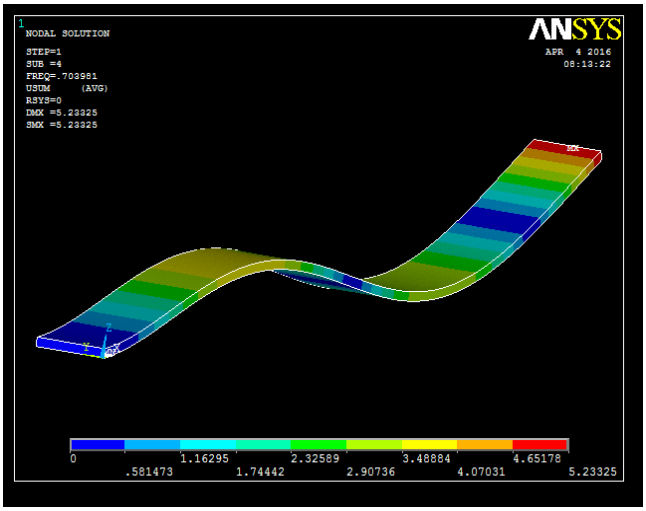

Fig 16: third mode shape of C-F PRP beam at 10% SiC.

Table 3: Comparison of natural frequencies obtained by analytical, FEA and Experimental methods for clamped-free boundary conditions.

% of SiC	Non-dimensional first natural frequency			Non-dimensional second natural frequency			Non-dimensional third natural frequency		
	Theoretical	FEA	Experimental	Theoretical	FEA	Experimental	Theoretical	FEA	Experimental
10%	0.993985	0.995	0.9772	0.98	0.9903	0.9525	0.99272	0.9937	0.9859
15%	0.96599	0.9675	0.9272	0.95	0.9592	0.9205	0.98167	0.9851	0.9535
20%	0.7725	0.7776	0.80273	0.77	0.7757	0.822	0.82081	0.8263	0.85
25%	0.73621	0.7502	0.71697	0.69	0.7017	0.6801	0.72857	0.7325	0.7083
30%	0.68651	0.6898	0.672	0.68	0.6899	0.7086	0.69262	0.6959	0.6755

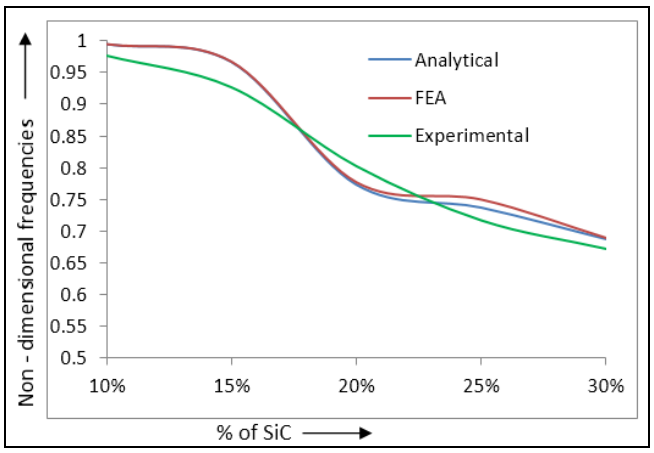

Fig 17: comparisons of first natural frequencies of Clamped-Free PRP beam.

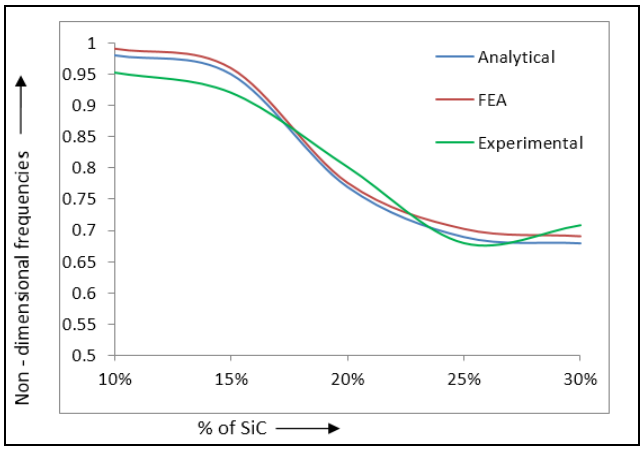

Fig 18: comparisons of first natural frequencies of Clamped-Free PRP beam.

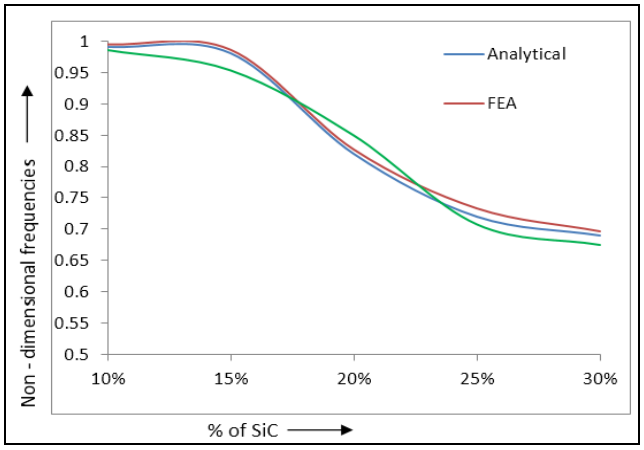

Fig 19: comparisons of first natural frequencies of Clamped-Free PRP beam.

6. Conclusions

Free vibration of PRP composite beams with varying the weight percentage of SiC by analytical method, FEA and experimental methods are studied. From the both methods vibration parameters (natural frequency and mode shapes of PRP composite beams are obtained. It is examined that the outcomes are varying 0% to 5% which may be considered as a good agreement. Further finite element analysis is carried out from this investigation; it is observed that the mode shapes and corresponding natural frequencies of PRP beam are different with respect to SiC weight percentage. Also by varying the SiC weight, the natural frequency and mode shape have significantly changed due to the change in the stiffness of PRP beam. The dynamic response (natural frequency and corresponding mode shape) achieved from the FEA are validated through the results of analytical and experimental methods. The results are in good agreement with error percentage within 5%.

7. References

1. Robert M. Jones, Mechanics of Composite Materials. McGraw-Hill Book Co, 1975.
2. Christensen RM. Mechanics of Composite Materials, 1979.
3. Tsai SW, Hahn HT. Introduction to Composite Materials, Technomic Publishing Co., 1980.
4. Hull D. An Introduction to Composite Materials, Cambridge University Press, 1981.
5. Halpin JC. Primer on Composite Materials: Analysis, Technomic Publishing Co., 1984.
6. Vinson JR, Sierakowski RL. The Behavior of Structures Composed of Composite Materials, Martinus Nijhoff Publishers, 1986.
7. Gibson RF. Principles of Composite Material Mechanics, McGraw-Hill Book Co. 1994.
8. Phillip BM, Enmanuel PG. Synthesis and characterization of layered silicate-epoxy nanocomposites, Chemical mater, 1994; 6:1719-1725.
9. Alexandre M, Dubois P. Polymer-layered silicate nano-composites Preparation Properties and uses of a new Polymer and composite materials, Materials Science and Engineering, 2000; 28:1-653.
10. Nathaniel C, Hassan M, Vijaya R, Reneé R, Shaik J. Synthesis & Mechanical Characterization of Carbon/Epoxy Composites Reinforced with SiC Nano Particles, NSTI-Nanotech, ISBN 0-9728422-9-2, 2004; 3:302-307.
11. Botelho EC, Costa ML, Rezende MC, Pardini LC. Effect of the hygrothermal conditioning on the mechanical properties of carbon fiber/epoxy composites, Proceedings of COBEM 2005, 18th International Congress of Mechanical Engineering, 2005, 6-11.
12. Suresha B, Ghandramohan G, Prakash JN, Balusamy V, Sankarnarayanasamy K. The Role of Fillers on friction and slide wear characterization & Engineering 2006; 5:87-101.
13. Wrobel G, Kaczmarczyk J, Stabik J, Rojek M. Numerical models of polymeric composite to simulate fatigue and ageing processes, Journal of Achievements in materials and Manufacturing Engineering. 2009; 34(1):31-38.
14. Muthirakkal S, Murthy HNRN, Krishna M, Rai KS, Karippal JJ, Hygrothermic Behaviour of Carbon/Vinylester, Glass/Vinylester, Carbon/Epoxy and Glass/Epoxy Composites, Iranian polymer Journal. 2010; 19(2):89-102.
15. Zhang G, Rashova Z, Karger-Kocsis T, Burkhart T. synergetic role of nano-scale short carbon fibers on the

mechanical properties of epoxy resin, express polymer Letters, 2011; 5(10):859-872.
16. Gao J, Li J, Benicewicz BC, Zhao S, Hillborg H, Schadler LS. The Mechanical Properties of Epoxy Composites Filled with Rubbery Copolymer Grafted SiO2, Polymers, 2012; 4:187-210.
17. Rojek M, Szymiczek M, Stabik J, Mezyk A, Jamroziak K, Krzystała E, *et al*. Composite materials with the polymeric matrix applied to ballistic shields, Journal of Achieves in Materials Science and Engineering. 2013; 63(1):26-35.
18. Begum K, Islam MA. Natural Fiber as a substitute to Synthetic Fiber in Polymer Composites, Research Journal of Engineering Sciences, 2013; 2(3):46-53.
19. Islam MS, Masoodi R, Rostami H. The Effect of Nanoparticles Percentage on Mechanical Behavior of Silica-Epoxy Nanocomposites, Journal of NanoScience. 2013; 275037:1-10.
20. Alhuthali AM, Low IM. Characterisation of Mechanical and Fracture Behaviour in Nano- Silicon Carbide Reinforced Vinyl-ester Nanocomposites, Department of Imaging and Applied Physics, Curtin University, GPO Box U1987, Perth, WA 6845, Australia
21. Benmansour N, Agoudjil B, Gherabli A, Kareche A, Boudenne A. Thermal and mechanical performance of natural mortar reinforcedwith date palm fibers for use as insulating materials in building, Energy and Buildings, 2014; 81:98-104,.
22. Mohan N, Mahesha CR, Raja R, Tribo-mechanical behaviour of SiC filled glass-epoxy composites at elevated temperatures, International Journal of Engineering, Science and Technology, 2014; 6(5): 44-56.
23. Arpitha GR, Sanjay MR, Naik LL, Yogesha B. Mechanical Properties of Epoxy Based Hybrid Composites Reinforced with Sisal/SIC/Glass Fibers, International Journal of Engineering Research and General Science. 2014; 2(5):398-405.
24. Sanjay MR, Arpitha GR, Yogesha B. Investigation on Mechanical Property Evaluation of Jute - Glass Fiber Reinforced Polyester, IOSR Journal of Mechanical and Civil Engineering. 2014; 11(4):50-57.
25. Chao C, Yongjun T, Yun S, Ye Zhigang X, Yang X, Xiaolin X, *et al*. High-performance epoxy/silica coated silver nanowire composites as under fill material for electronic packaging. Composites Science and Technology, 2014; 105:80-85.
26. Jena PC, Parhi DR, Pohit G. Faults detection of a single cracked beam by theoretical and experimental analysis using vibration signatures, Journal of Mechanical and Civil Engineering. 2012; 4(3):1-18.
27. Parhi Dayal R, Jena PC, Pohit G. Faults Recognition of a Single Cracked Beam with Analytical and Experimental Methods by using Vibration Signatures. International Journal of Applied Artificial Intelligence in Engineering System, 2014; 6(1):63-76.
28. Jena PC, Parhi Dayal R, Pohit G, Theoretical. Numerical (FEM) and Experimental Analysis of composite cracked beams of different boundary conditions using vibration mode shape curvatures, International Journal of Engineering and Technology. 2014; 6(2):509-518.
29. Jena PC, Parhi DR, Pohit G, Samal BP. Crack Assessment by FEM of AMMC Beam Produced by Modified Stir Casting Method, Journal of Materials Today: Proceedings. 2015, 2267-2276.
30. ANSYS user manual release, 2013.